ACS APPLIED MATERIALS & INTERFACES

Research Article

Cite This: ACS Appl. Mater. Interfaces 2018, 10, 30946−30951

www.acsami.org

Biocompatible Single-Chain Polymer Nanoparticles for Drug Delivery—A Dual Approach

A. Pia P. Kröger,[†] Naomi M. Hamelmann,[†] Alberto Juan,[†,‡] Saskia Lindhoud,[§] and Jos M. J. Paulusse*[,†,∥]

[†]Department of Biomolecular Nanotechnology, MESA+ Institute for Nanotechnology and TechMed Institute for Health and Biomedical Technologies, Faculty of Science and Technology, [‡]Department of Molecular NanoFabrication, MESA+ Institute for Nanotechnology, Faculty of Science and Technology, and [§]Department of Nanobiophysics, MESA+ Institute for Nanotechnology, Faculty of Science and Technology, University of Twente, P.O. Box 217, 7500 AE Enschede, The Netherlands

[∥]Department of Nuclear Medicine and Molecular Imaging, University Medical Center Groningen, P.O. Box 30.001, 9700 RB Groningen, The Netherlands

Supporting Information

ABSTRACT: Single-chain polymer nanoparticles (SCNPs) are protein-inspired materials based on intramolecularly cross-linked polymer chains. We report here the development of SCNPs as uniquely sized nanocarriers that are capable of drug encapsulation independent of the polarity of the employed medium. Synthetic routes are presented for SCNP preparation in both organic and aqueous environments. Importantly, the SCNPs in organic media were successfully rendered water soluble, resulting in two complementary pathways toward water-soluble SCNPs with comparable resultant physicochemical characteristics. The solvatochromic dye Nile red was successfully encapsulated inside the SCNPs following both pathways, enabling probing of the SCNP interior. Moreover, the antibiotic rifampicin was encapsulated in organic medium, the loaded nanocarriers were rendered water soluble, and a controlled release of rifampicin was evidenced. The absence of discernible cytotoxic effects and promising cellular uptake behavior bode well for the application of SCNPs in controlled therapeutics delivery.

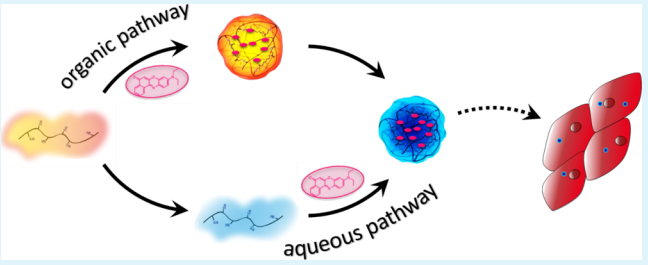

KEYWORDS: *single-chain polymer nanoparticles, controlled drug delivery, thiol-Michael addition, thiol polymers, drug encapsulation*

INTRODUCTION

Single-chain polymer nanoparticles (SCNPs) are prepared through exclusive intramolecular cross-linking of polymer chains and have been developed as promising uniquely sized nanoparticle systems over the past 2 decades.[1,2] The intramolecular chain collapse gives access to extremely small polymeric nanoparticles (∼10 nm), unparalleled by other means of preparation. In view of anticipated applications as drug carriers and protein-mimicking systems, a number of strategies to prepare the water-soluble SCNPs has been brought into focus in the recent past, including the postformation functionalization of carboxylic acid polymers with benzyl or *tert*-butyloxycarbonyl protecting groups[3,4] or alternatively the use of amphiphilic copolymers such as poly(*N*-isopropylacrylamide), poly(2-(*N*,*N*-dimethylamino)ethyl methacrylate), and polyethylene glycol.[5−7] Several strategies have been developed to covalently cross-link the polymers intramolecularly directly in water, for example, via amidation of glutamic acid,[8] via thiol-Michael addition,[9] or via tetrazole−ene cycloaddition.[10]

To investigate the potential of SCNPs as drug carriers, dye molecules, as well as therapeutic cargos such as doxorubicin, have been successfully encapsulated into the SCNPs.[11−13] To our knowledge, a nanoparticle system for therapeutics encapsulation independent of their lipophilicity with appreciable encapsulation efficiencies is still pending.

We recently demonstrated the rapid and efficient synthesis of SCNPs via a phosphine-induced thiol-Michael cross-linking in an organic medium.[14] The thiol-Michael reaction can be readily performed in the organic medium without the need for a high temperature or metal catalysts but also takes place in a basic aqueous medium and therefore poses little restriction with respect to the reaction medium.[15,16]

Herein, we report on the dual-pathway synthesis in both the aqueous and organic phases of water-soluble SCNPs, enabling a polarity-independent therapeutics encapsulation and a subsequent release under physiologically relevant conditions (Scheme 1). The cytotoxic effects of the SCNPs are evaluated on human cervical cancer (HeLa) and human brain endothelial (hCMEC/D3) cells. hCMEC/D3 cells are further explored as a model for

Received: May 8, 2018
Accepted: August 28, 2018
Published: August 28, 2018

Scheme 1. Dual-Pathway Synthesis of SCNPs via Thiol-Michael Addition[a]

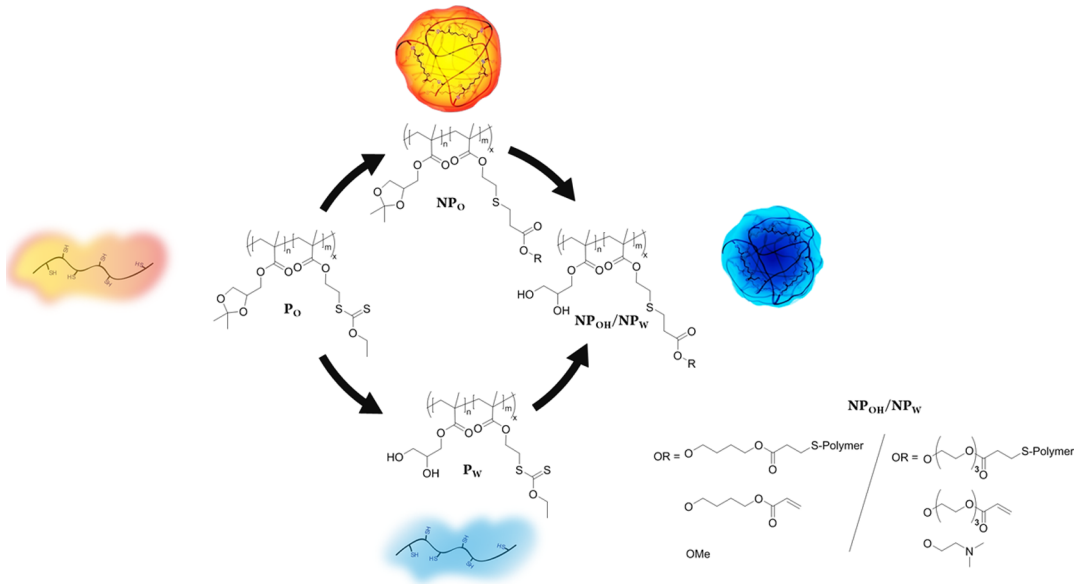

[a]Starting from the polymer $\mathbf{P_O}$ (soluble in organic solvents), nanoparticles are prepared in dichloromethane ($\mathbf{NP_O}$, organic pathway), or the polymer is hydrolyzed to its water-soluble analogue ($\mathbf{P_W}$) to serve as a precursor for nanoparticle formation in an aqueous solvent ($\mathbf{NP_W}$, aqueous pathway). Nanoparticles $\mathbf{NP_O}$ are also hydrolyzed to render them water soluble ($\mathbf{NP_{OH}}$).

drug transport to the central nervous system in cellular uptake studies with SCNPs.

EXPERIMENTAL SECTION

General Procedures for Thiol Aminolysis of the Copolymers. The copolymer (500 mg) (i.e., 0.30 mmol equiv thiol monomer) was dissolved in 10 mL of the solvent [tetrahydrofuran (THF) for the organic route and dimethyl sulfoxide (DMSO) for the aqueous route] and purged with nitrogen for 10 min in a sealed round-bottom flask. Under nitrogen flow, hydrazine monohydrate (29 μL, 0.60 mmol, 2.00 equiv) was added. The solution was stirred for 60 min in the case of $\mathbf{P_O}$ and 30 min for $\mathbf{P_W}$. The copolymer solutions were filtered and immediately used in nanoparticle formation.

P$_O$. ^{1}H NMR (400 MHz, $CDCl_3$) δ_H: 4.40−4.22 (br, CH), 4.14−3.65 (br, m, CH_2), 2.80−2.67 (br, CH_2), 2.12−1.71 (br), 1.69−1.45 (br), 1.48−1.32 (d, $(CH_3)_2$), 1.14−0.78 (br).

P$_W$. ^{1}H NMR (400 MHz, DMSO-d_6) δ_H: 4.92 (s, OH), 4.68 (s, OH), 4.33−4.22 (br, CH_2), 4.05−3.16 (br, m, CH, CH_2), 2.11−1.56 (br), 1.17−0.54 (br).

Nanoparticle Formation in an Organic Solvent ($\mathbf{NP_O}$). The nanoparticle formation in an organic solvent was performed as described earlier.[14] In brief, 1,4-butanediol diacrylate (11.9 μL, 0.25 mmol, 1.00 equiv) and tri(*n*-butyl)phosphine (11.0 μL, 0.05 mmol, 0.2 equiv) were added to 100 mL of nitrogen-purged dichloromethane. The solution of deprotected $\mathbf{P_O}$ (500 mg, 0.25 mmol equiv thiol monomer) in THF (10 mL) was dropwise added to the continuously stirred cross-linker solution over 30 min. After 3 h of stirring, a large excess of methyl acrylate (1.5 mL, 14 mmol) was added and the solution was left stirring overnight. Subsequently, the solution was filtered and concentrated under a reduced pressure. Finally, the nanoparticles were precipitated to *n*-heptane (~200 mg).

NP$_O$. ^{1}H NMR (400 MHz, $CDCl_3$) δ_H: 4.40−4.22 (br, CH), 4.14−3.65 (br, m, CH_2), 2.88−2.42 (br, CH_2), 2.12−1.71 (br), 1.69−1.45 (br), 1.48−1.32 (d, $(CH_3)_2$), 1.14−0.78 (br).

Hydrolysis of Copolymer Xanthate Methacrylate−Solketal Methacrylate ($\mathbf{P_w}$) and Nanoparticles ($\mathbf{NP_{OH}}$). To a solution of $\mathbf{P_O}$ or $\mathbf{NP_O}$ in THF, an aqueous HCl solution (8 M) was slowly added until a turbid solution was obtained. The mixture was stirred for 2 h and subsequently dialyzed against demi-water and filtered. Freeze-drying yielded a pale pink lyophilizate of $\mathbf{P_W}$ and a white lyophilizate of $\mathbf{NP_{OH}}$.

P$_W$. ^{1}H NMR (400 MHz, DMSO-d_6) δ_H: 4.92 (s, OH), 4.68 (s, OH, CH_2), 4.25−3.16 (br, m, CH, CH_2), 2.11−1.56 (br), 1.39 (s, CH_3), 1.17−0.54 (br).

NP$_{OH}$. ^{1}H NMR (400 MHz, DMSO-d_6) δ_H: 4.92 (s, OH), 4.68 (s, OH, CH_2), 4.17−3.57 (br, m, CH, CH_2), 2.82−2.57 (br, CH_2), 2.11−1.56 (br), 1.55−1.32 (br), 1.17−0.54 (br).

Nanoparticle Formation in an Aqueous Solution ($\mathbf{NP_W}$). Carbonate−bicarbonate buffer (100 mL, CBB, 0.1 M sodium carbonate/sodium decarbonate, pH 9−10) was purged with nitrogen prior to the addition of poly(ethylene glycol)diacrylate (58 g/mol, 73.0 μL, 0.30 mmol, 1.00 equiv) and tris(2-carboxyethyl)phosphine (TCEP, 15.6 mg, 0.05 mmol, 0.2 equiv). The solution of deprotected copolymer $\mathbf{P_W}$ (500 mg, 0.30 mmol equiv thiol monomer) in DMSO (10 mL) was dropwise added to the continuously stirred cross-linker solution over 30 min. After 4 h of stirring, 2.2 mL of dimethylaminoethyl acrylate (DMAEA) (16 mmol) was added, and the solution was left stirring overnight. Subsequently, the solution was filtered and concentrated under a reduced pressure. The obtained solution was dialyzed against demi-water, filtered, and freeze-dried to obtain a white lyophilizate (~300 mg).

NP$_W$. ^{1}H NMR (400 MHz, DMSO-d_6) δ_H: 6.41−4.29 (CH), 6.27−6.12 (CH), 6.03−5.85 (CH), 4.92 (s, OH), 4.68 (s, OH), 4.31−3.03 (br, m, CH, CH_2), 2.88−2.59 (br, m, CH_2), 2.11−1.56 (br), 1.17−0.54 (br).

Nile Red Encapsulation ($\mathbf{NP_W}$-NR and $\mathbf{NP_{OH}}$-NR). For the encapsulation of Nile red (NR) in SCNPs, NR was added during the above-described SCNP formation procedure. For the formation in an organic solvent, NR was added to the dichloromethane phase (0.4 mg/mL), and during the formation in the aqueous solvent, NR was added to the DMSO phase (1 mg/mL) as NR is barely soluble in water. Subsequently to the reaction, the reaction mixtures were concentrated. For $\mathbf{NP_O}$-NR, the nanoparticles were hydrolyzed through the addition of 10 mL of aqueous HCl solution (8 M). Both nanoparticle systems, $\mathbf{NP_W}$-NR and $\mathbf{NP_{OH}}$-NR, were dialyzed against water followed by filtration and freeze-drying to obtain a dark purple lyophilizate. During dialysis against water, no visible amounts of NR were dialyzed out, although the purple precipitate formed, which was filtered off. The samples were dissolved in dimethylformamide (DMF) and analyzed by gel permeation chromatography (GPC) coupled with a fluorescence detector. For emission spectra, the eluents were excited at 550 nm, and for excitation spectra, the emission was detected at 615 nm.

DOI: 10.1021/acsami.8b07450
ACS Appl. Mater. Interfaces 2018, 10, 30946−30951

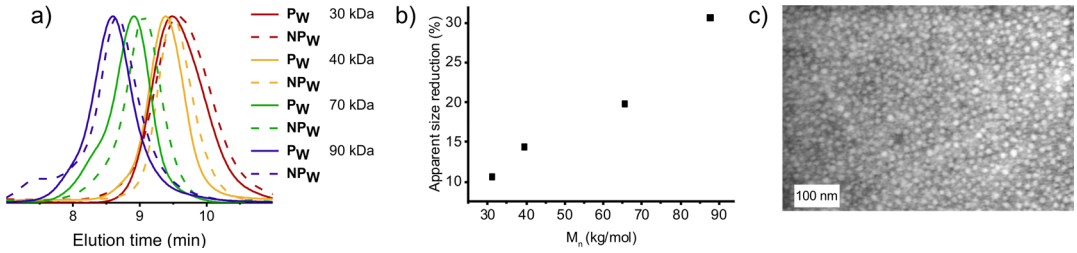

Figure 1. (a) Overlay of GPC traces for the water-soluble copolymer precursors $\mathbf{P_W}$ (solid) with different chain lengths and their corresponding nanoparticles $\mathbf{NP_W}$ (dotted); (b) size reduction of $\mathbf{NP_W}$ vs number-averaged molecular weight of $\mathbf{P_W}$; (c) STEM image of $\mathbf{NP_W}$ (30 kDa).

Rifampicin Encapsulation ($\mathbf{NP_{OH}}$-Rif). The encapsulation of rifampicin (Rif) in $\mathbf{NP_{OH}}$ was performed analog to the encapsulation with 1 mg/mL Rif in dichloromethane. The product was dissolved in DMF and analyzed via a GPC-coupled photodiode array detector.

Rif Release. The drug release from $\mathbf{NP_{OH}}$-**Rif** was evaluated according to an earlier described procedure.[17] In brief, 18 samples of 1 mL of each $\mathbf{NP_{OH}}$-**Rif** (1 g/L) and Rif (0.1 g/L) were dialyzed against 2 L of water. After 1, 2, 4, 6, 10, 22, and 48 h, the water was refreshed, and after 2, 4, 6, 10, 22, and 48 h, three bags of each sample were removed and measured. The Rif concentration was determined with its UV−vis absorbance at 344 nm.

RESULTS AND DISCUSSION

Copolymers of solketal methacrylate monomer, to provide water solubility, and xanthate methacrylate (**XMA**) monomer, to provide thiol moieties for Michael cross-linking, were prepared via reversible addition−fragmentation chain transfer polymerization. The incorporation ratios of the obtained copolymers ($\mathbf{P_O}$) with molecular weights between 30 and 70 kg/mol and low polydispersities (PDI ≈ 1.10) matched well with the feed ratios of 10% of **XMA**.

Prior to SCNP formation in the organic solvent, xanthate moieties were deprotected via thiol aminolysis with hydrazine. ^{1}H NMR spectroscopy confirmed full deprotection within 30 min through the disappearance of the ethyl xanthate signals. $\mathbf{P_O}$ was cross-linked via thiol-Michael addition under continuous addition of the deprotected polymer to a cross-linker solution containing a phosphine initiator as described previously.[14] The residual thiol moieties were passivated by excess methyl acrylate, and product nanoparticles ($\mathbf{NP_O}$) were isolated via precipitation. Separate signals corresponding to the methyl group of methyl acrylate at 3.71 ppm and to the butyl ester moiety of butanediol diacrylate at 1.75 ppm are identified in the ^{1}H NMR spectrum (Figure S1). Although both signals overlap to some extent with other signals, approximately half of the thiols react with the cross-linker. As ^{1}H NMR spectroscopy does not allow distinguishing between intra- and intermolecular reactions, GPC was employed (Table S5 and Figure S10). The comparison of the elution times of polymer $\mathbf{P_O}$ and nanoparticle $\mathbf{NP_O}$ revealed a relative size reduction of 23%, indicating a chain collapse through intramolecular cross-linking.

To achieve water-soluble nanoparticles directly from the polymers, the above-described SCNP formation process was also carried out in an aqueous medium. To render polymer $\mathbf{P_O}$ water soluble, the solketal moieties on the polymer were hydrolyzed to the corresponding diglycol groups under acidic conditions to achieve a water-soluble copolymer ($\mathbf{P_W}$). Complete hydrolysis was confirmed by ^{1}H NMR spectroscopy and by Fourier transform infrared (FT-IR) spectroscopy (Figures S1 and S2). As the thiol-Michael addition in an aqueous environment proceeds most efficiently under basic conditions,[16] SCNP formation was performed with TCEP as an initiator in CBB (0.1 M, pH 9) with oligo ethylene glycol diacrylate (M_n = 258 Da) as a water-soluble cross-linker and *N*,*N*-DMAEA as an endcapper. Successful thiol-Michael addition was confirmed by ^{1}H NMR spectroscopy (Figure S1). The GPC measurements on both polymers $\mathbf{P_W}$ and nanoparticles $\mathbf{NP_W}$ revealed relative size reductions of 10−30% depending on the polymer length. Longer polymers result in larger size reductions (Table S1 and Figure 1a,b), presumably because of the higher number of cross-links. The dependency of nanoparticle size on the precursor polymer is an indication of SCNP formation and is in line with our previous findings for thiol-Michael addition-based SCNPs.[14]

Dynamic light scattering (DLS) measurements revealed comparable sizes for all $\mathbf{NP_W}$ nanoparticles, around 4.0 nm in hydrodynamic radius (r_H), whereas the sizes of the polymer precursors depend on the molecular weight, ranging from 3.6 to 7.2 nm, hence demonstrating a higher relative size reduction for longer polymers (Table S1 and S2). Diffusion-ordered spectroscopy (DOSY) NMR spectroscopy experiments further support the DLS measurements, evidencing a reduction in r_H from 8.8 to 7.9 nm in DMSO (Figure S4). Small-angle X-ray scattering (SAXS) experiments confirm a size reduction by the cross-linker-induced chain collapse and a radius of gyration of 3.9 nm for $\mathbf{NP_W}$ (Figure S5 and Table S3). Fitted SAXS measurements further reveal a decrease in the scaling exponent ν in DMSO when comparing the polymer (0.58) with the SCNPs (0.44). As described by the Flory exponent, the polymer corresponds to a self-avoiding chain (ν = 0.6), while the SCNPs approach the behavior of coiled, spherical structures (ν = 1/3).[18,19] Further analysis with a triple-detector GPC system [multiangle light scattering (MALS), refractive index, and viscometer] in DMF revealed a decrease in the hydrodynamic radius and intrinsic viscosity upon cross-linking while molecular weight remained unaltered (Table S4).

Scanning transmission electron microscopy (STEM) imaging of negatively stained $\mathbf{NP_W}$ shows uniform round objects ca. 6.5 nm in radius (Figure 1c). This size is larger than the sizes determined by DLS and SAXS, but in agreement with the particles in a dried state.[14,20]

Hydrolysis of the solketal moieties of the nanoparticle $\mathbf{NP_O}$ was performed to obtain the water-soluble SCNPs $\mathbf{NP_{OH}}$ via the organic pathway. Because hydrolysis requires relatively strong acidic conditions, the integrity of the intramolecular cross-links formed during the thiol-Michael addition needs to be verified. Upon comparing the hydrolyzed nanoparticles $\mathbf{NP_{OH}}$ with the nanoparticles $\mathbf{NP_W}$, based on the water-soluble precursor polymer $\mathbf{P_W}$, both ^{1}H NMR and FT-IR measurements show comparable spectra, and no signs indicating the formation of carboxylic acids due to the hydrolysis of ester bonds were observed (Figures S1 and S9). The molecular weights of the hydrolyzed polymer $\mathbf{P_W}$ and the nanoparticle $\mathbf{NP_{OH}}$ are in the

DOI: 10.1021/acsami.8b07450
ACS Appl. Mater. Interfaces 2018, 10, 30946−30951

same range as the molecular weights observed for the corresponding polymer $\mathbf{P_O}$ and the nanoparticle $\mathbf{NP_O}$ before hydrolysis, with an apparent size reduction of 11% (Figure S10 and Table S5).

In order to probe the SCNP formation process, the solvatochromic dye NR was encapsulated by carrying out SCNP formation in the presence of NR, via both the organic and the aqueous pathways. NR is poorly soluble and barely fluorescent in water; however, upon encapsulation, the fluorescence intensity of the lyophilized NR-containing SCNPs ($\mathbf{NP_{OH}}$-**NR**) in water increased markedly, while the emission blue-shifted in comparison to free NR, indicating a more hydrophobic environment of NR.[21,22] Successful encapsulation of NR in both $\mathbf{NP_W}$ and $\mathbf{NP_{OH}}$ was evidenced by the coelution of nanoparticles and NR in GPC measurements (Figures 2a and S10b). Further, the fluorescence spectra of the

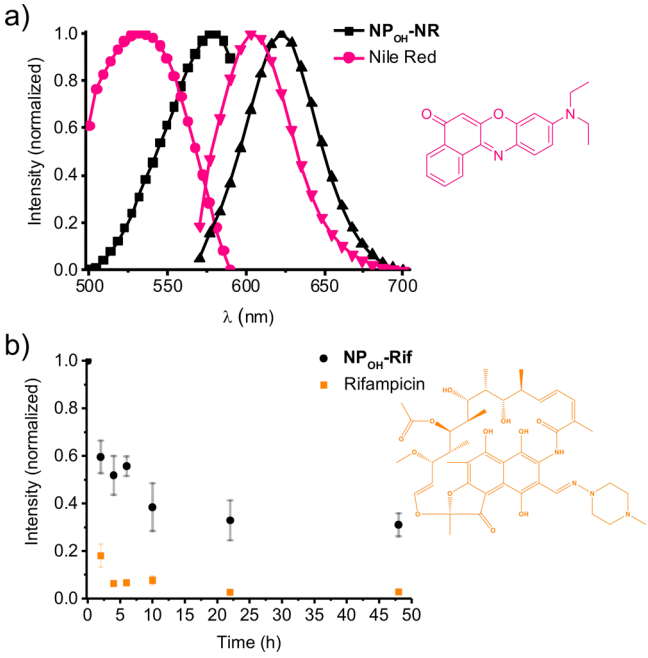

Figure 2. (a) Fluorescence spectra of free (pink) and SCNP-encapsulated (black) NR eluting from GPC in DMF (excitation at 550 nm, emission at 615 nm). (b) Release of Rif from SCNPs by measuring UV−vis absorption at 334 nm.

encapsulated NR are red-shifted, demonstrating that NR is located in a more hydrophilic environment than DMF. The red shift is more pronounced for NPs prepared via the organic pathway ($\mathbf{NP_{OH}}$) most likely because of a higher NR concentration during the formation. It should be noted that NR has only limited water solubility, which is why no release study was performed for NR.

In order to evaluate SCNPs as drug carriers, Rif, a broad-spectrum antibiotic with an excellent bactericidal activity, particularly used in the fight against tuberculosis and pneumococcal meningitis, was encapsulated in $\mathbf{NP_{OH}}$ nanoparticles.[23,24] GPC analysis revealed the coelution of Rif and $\mathbf{NP_{OH}}$ nanoparticles, as observed by a UV−vis absorbance band characteristic of the encapsulated Rif (Figure S13).[25] UV−vis spectroscopy indicates that the $\mathbf{NP_{OH}}$-**Rif** nanoparticles contain approximately 16 wt % Rif, which corresponds to an entrapment efficiency of 81%. It should be noted that not all free Rif can be removed without also removing the cargo Rif. Subsequently, drug release was assessed through dialysis of the obtained $\mathbf{NP_{OH}}$-**Rif** nanoparticles and tracking Rif release via UV−vis measurements. After a burst release of Rif in the first 2 h (40% release), a sustained release of Rif from $\mathbf{NP_{OH}}$-**Rif** was observed, as compared to a Rif control solution (Figure 2b). Although the majority of Rif (80%) of the control solution was dialyzed out at the first time point (2 h), the $\mathbf{NP_{OH}}$-**Rif** solution still contained over 60% of the original Rif content. Electrospray ionization mass spectrometry confirmed that Rif remained unaltered after encapsulation, acid hydrolysis, and release (Figure S14).

An important prerequisite for use as a drug carrier is biocompatibility. Both polymer **P2** and nanoparticle $\mathbf{NP_W}$ were evaluated for cytotoxicity with a cell viability assay on HeLa (Figure S6) and on hCMEC/D3 cells (Figures 3 and S7).

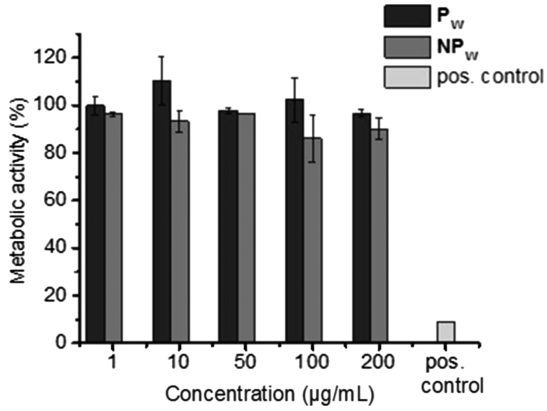

Figure 3. Metabolic activity of hCMEC/D3 cells after incubation with $\mathbf{P_W}$ and $\mathbf{NP_W}$ for 48 h.

Both cell lines maintained their metabolic activities after incubation with $\mathbf{P_W}$, $\mathbf{NP_W}$, and $\mathbf{NP_{OH}}$ for 48 h at concentrations of up to 500 μg/mL. Moreover, no discernible influence on cell morphologies or confluency of the hCMEC/D3 cells was observed with phase contrast microscopy (Figure S8).

To facilitate further cell studies, fluorescent labeling of the nanoparticles was investigated. Conjugation of *N*-methylanthraniloyl onto diglycol moieties is an efficient and low-cost method and is commonly employed in the labeling of biomolecules, such as nucleotides and peptides. On the other hand, 5-(4,6-dichlorotriazinyl)aminofluorescein (DTAF) is an effective reagent to label both amine and alcohol moieties of biopolymers at a basic pH.[26,27] Successful addition of the labels to the nanoparticles was confirmed by GPC coupled with a fluorescence detector (Figure S15); however, DTAF turned out to be the more suitable label because of higher contrast with cell autofluorescence. A concentration-dependent cellular uptake of DTAF-labeled $\mathbf{NP_W}$ by hCMEC/D3 endothelia cells was clearly observed by confocal laser scanning microscopy (CLSM) and quantified with fluorescence-activated cell sorting (FACS), and even at the lowest concentration (5 μg/mL), the cellular uptake is observed (Figures 4, S16, and S17).

A common issue with the cell uptake of nanoparticles is degradation by lysosomes.[28] Importantly, lysosome costaining of hCMEC/D3 cells did not reveal the colocalization of nanoparticles with lysosomes (Figure S18b), although the CLSM images suggest vesiculation of the nanoparticles and hence uptake via endocytosis. The uptake mechanism and final destination of the SCNPs are currently under investigation. Because the nanoparticles are able to bypass the lysosomes, their

DOI: 10.1021/acsami.8b07450
ACS Appl. Mater. Interfaces 2018, 10, 30946−30951

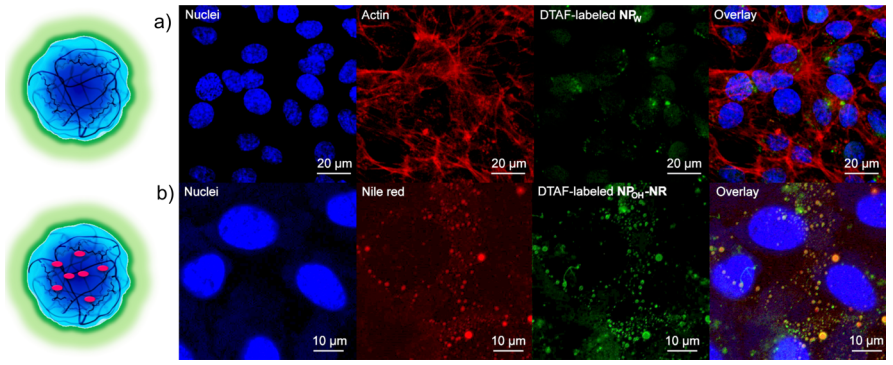

Figure 4. CLSM images of hCMEC/D3 cells (a) after incubation with DTAF-labeled $\mathbf{NP_W}$ (green) for 20 h stained with Alexa Fluor 647 phalloidin (red) and 4′,6-diamidino-2-phenylindole (DAPI) (blue); (b) after incubation with DTAF-labeled, NR-loaded $\mathbf{NP_{OH}}$ for 20 h stained with DAPI (blue).

ability as a drug delivery agent was further investigated by employing fluorescent NR as a model compound. DTAF-labeled $\mathbf{NP_{OH}}$**-NR** was chosen because of the higher drug loading obtained via the organic pathway. As observed in Figure 4, NR and DTAF are colocalized in the cells. It should be noted that the sample contains a non-negligible amount of non-encapsulated NR. Nevertheless, the colocalization of cargo and nanoparticles hint toward SCNPs as a successful drug delivery system. As the aforementioned release studies with NR proved unsuccessful, the release inside the cytosol may be hampered as well.

CONCLUSIONS

Making use of thiol-Michael cross-linking and solketal as an adaptable moiety, both organic and aqueous pathways toward water-soluble SCNPs have been presented. A combination of characterization methods demonstrated the formation of well-defined particles approximately 3−5 nm in radius. Cell viability studies demonstrated no cytotoxicity effect even at elevated concentrations. Furthermore, uptake by hCMEC/D3 cells was demonstrated with DTAF-labeled SCNPs. In combination with drug encapsulation and release, this SCNP system offers with the dual-preparation pathway—the opportunity to encapsulate drug molecules irrespective of their lipophilicity. These results highlight the potential of SCNPs as a biomaterial and in particular as a drug delivery system to brain tissues. Current efforts are focused on the in vivo evaluation of these promising drug carriers.

ASSOCIATED CONTENT

Supporting Information

The Supporting Information is available free of charge on the ACS Publications website at DOI: 10.1021/acsami.8b07450.

Materials and methods, Ellman's assay, cell toxicity/cellular uptake experiments, ^{1}H NMR, FT-IR, DOSY-NMR, SAXS, GPC, electrospray ionization mass spectrometry, fluorescence, UV−vis absorption, and FACS measurements (PDF)

AUTHOR INFORMATION

Corresponding Author

*E-mail: j.m.j.paulusse@utwente.nl.

ORCID

A. Pia P. Kröger: 0000-0001-7031-0598
Naomi M. Hamelmann: 0000-0002-7126-4818
Alberto Juan: 0000-0002-4159-9772
Saskia Lindhoud: 0000-0002-4164-0763
Jos M. J. Paulusse: 0000-0003-0697-7202

Notes

The authors declare no competing financial interest.

ACKNOWLEDGMENTS

J.M.J.P. and A.P.P.K. gratefully acknowledge the funding from the Netherlands Organization for Health Research and Development (ZonMw, project number 733050304). S.L. and J.M.J.P. thank the Diamond Light Source for the beam time (SM16050-1) and Dr. Katsuaki Inoue and Dr. Robert Rambo for their involvement in the SAXS experiments. Mark Smithers is thanked for the STEM measurements and Jonathan Wilbrink for support with the fluorescence measurements. The authors further thank Marc Ankone for the support in the synthesis and Maaike Schotman and Regine van der Hee for the support in cell experiments. Furthermore, the team of Wyatt Technology Europe GmbH is thanked for the MALS analysis.

REFERENCES

(1) Gonzalez-Burgos, M.; Latorre-Sanchez, A.; Pomposo, J. A. Advances in Single Chain Technology. *Chem. Soc. Rev.* **2015**, *44*, 6122−6142.

(2) Lyon, C. K.; Prasher, A.; Hanlon, A. M.; Tuten, B. T.; Tooley, C. A.; Frank, P. G.; Berda, E. B. A brief user's guide to single-chain nanoparticles. *Polym. Chem.* **2015**, *6*, 181−197.

(3) Croce, T. A.; Hamilton, S. K.; Chen, M. L.; Muchalski, H.; Harth, E. Alternative o-Quinodimethane Cross-Linking Precursors for Intramolecular Chain Collapse Nanoparticles. *Macromolecules* **2007**, *40*, 6028−6031.

(4) Perez-Baena, I.; Loinaz, I.; Padro, D.; García, I.; Grande, H. J.; Odriozola, I. Single-Chain Polyacrylic Nanoparticles with Multiple Gd(Iii) Centres as Potential MRI Contrast Agents. *J. Mater. Chem.* **2010**, *20*, 6916−6922.

(5) Ormategui, N.; García, I.; Padro, D.; Cabañero, G.; Grande, H. J.; Loinaz, I. Synthesis of single chain thermoresponsive polymer nanoparticles. *Soft Matter* **2012**, *8*, 734−740.

(6) Wen, J.; Zhang, J.; Zhang, Y.; Yang, Y.; Zhao, H. Controlled Self-Assembly of Amphiphilic Monotailed Single-Chain Nanoparticles. *Polym. Chem.* **2014**, *5*, 4032−4038.

(7) Lambert, R.; Wirotius, A.-L.; Taton, D. Intramolecular Quaternization as Folding Strategy for the Synthesis of Catalytically Active Imidazolium-Based Single Chain Nanoparticles. *ACS Macro Lett.* **2017**, *6*, 489−494.

(8) Radu, J. É. F.; Novak, L.; Hartmann, J. F.; Beheshti, N.; Kjøniksen, A.-L.; Nyström, B.; Borbély, J. Structural and Dynamical Character-

DOI: 10.1021/acsami.8b07450
ACS Appl. Mater. Interfaces 2018, 10, 30946−30951

ization of Poly-Gamma-Glutamic Acid-Based Cross-Linked Nanoparticles. *Colloid Polym. Sci.* **2008**, *286*, 365−376.
(9) Gracia, R.; Marradi, M.; Cossío, U.; Benito, A.; Pérez-San Vicente, A.; Gómez-Vallejo, V.; Grande, H.-J.; Llop, J.; Loinaz, I. Synthesis and Functionalization of Dextran-Based Single-Chain Nanoparticles in Aqueous Media. *J. Mater. Chem. B* **2017**, *5*, 1143−1147.
(10) Heiler, C.; Offenloch, J. T.; Blasco, E.; Barner-Kowollik, C. Photochemically Induced Folding of Single Chain Polymer Nanoparticles in Water. *ACS Macro Lett.* **2017**, *6*, 56−61.
(11) Song, C.; Li, L.; Dai, L.; Thayumanavan, S. Responsive single-chain polymer nanoparticles with host-guest features. *Polym. Chem.* **2015**, *6*, 4828−4834.
(12) Ryu, J.-H.; Chacko, R. T.; Jiwpanich, S.; Bickerton, S.; Babu, R. P.; Thayumanavan, S. Self-Cross-Linked Polymer Nanogels: A Versatile Nanoscopic Drug Delivery Platform. *J. Am. Chem. Soc.* **2010**, *132*, 17227−17235.
(13) Sanchez-Sanchez, A.; Akbari, S.; Moreno, A. J.; Lo Verso, F.; Arbe, A.; Colmenero, J.; Pomposo, J. A. Design and Preparation of Single-Chain Nanocarriers Mimicking Disordered Proteins for Combined Delivery of Dermal Bioactive Cargos. *Macromol. Rapid Commun.* **2013**, *34*, 1681−1686.
(14) Kröger, A. P. P.; Boonen, R. J. E. A.; Paulusse, J. M. J. Well-defined single-chain polymer nanoparticles via thiol-Michael addition. *Polymer* **2017**, *120*, 119−128.
(15) Hoyle, C. E.; Lowe, A. B.; Bowman, C. N. Thiol-Click Chemistry: A Multifaceted Toolbox for Small Molecule and Polymer Synthesis. *Chem. Soc. Rev.* **2010**, *39*, 1355−1387.
(16) Li, G.-Z.; Randev, R. K.; Soeriyadi, A. H.; Rees, G.; Boyer, C.; Tong, Z.; Davis, T. P.; Becer, C. R.; Haddleton, D. M. Investigation into Thiol-(Meth)Acrylate Michael Addition Reactions Using Amine and Phosphine Catalysts. *Polym. Chem.* **2010**, *1*, 1196−1204.
(17) Ekkelenkamp, A. E.; Jansman, M. M. T.; Roelofs, K.; Engbersen, J. F. J.; Paulusse, J. M. J. Surfactant-Free Preparation of Highly Stable Zwitterionic Poly(Amido Amine) Nanogels with Minimal Cytotoxicity. *Acta Biomater.* **2016**, *30*, 126−134.
(18) Pomposo, J. A.; Perez-Baena, I.; Lo Verso, F.; Moreno, A. J.; Arbe, A.; Colmenero, J. How Far Are Single-Chain Polymer Nanoparticles in Solution from the Globular State? *ACS Macro Lett.* **2014**, *3*, 767−772.
(19) ter Huurne, G. M.; Gillissen, M. A. J.; Palmans, A. R. A.; Voets, I. K.; Meijer, E. W. The Coil-to-Globule Transition of Single-Chain Polymeric Nanoparticles with a Chiral Internal Secondary Structure. *Macromolecules* **2015**, *48*, 3949−3956.
(20) Berda, E. B.; Foster, E. J.; Meijer, E. W. Toward Controlling Folding in Synthetic Polymers: Fabricating and Characterizing Supramolecular Single-Chain Nanoparticles. *Macromolecules* **2010**, *43*, 1430−1437.
(21) Deye, J. F.; Berger, T. A.; Anderson, A. G. Nile Red as a Solvatochromic Dye for Measuring Solvent Strength in Normal Liquids and Mixtures of Normal Liquids with Supercritical and Near Critical Fluids. *Anal. Chem.* **1990**, *62*, 615−622.
(22) Artar, M.; Terashima, T.; Sawamoto, M.; Meijer, E. W.; Palmans, A. R. A. Understanding the Catalytic Activity of Single-Chain Polymeric Nanoparticles in Water. *J. Polym. Sci., Part A: Polym. Chem.* **2014**, *52*, 12−20.
(23) Campbell, E. A.; Korzheva, N.; Mustaev, A.; Murakami, K.; Nair, S.; Goldfarb, A.; Darst, S. A. Structural Mechanism for Rifampicin Inhibition of Bacterial RNA Polymerase. *Cell* **2001**, *104*, 901−912.
(24) Martínez-Lacasa, J.; Cabellos, C.; Martos, A.; Fernández, A.; Tubau, F.; Viladrich, P. F.; Liñares, J.; Gudiol, F. Experimental Study of the Efficacy of Vancomycin, Rifampicin and Dexamethasone in the Therapy of Pneumococcal Meningitis. *J. Antimicrob. Chemother.* **2002**, *49*, 507−513.
(25) Ribeiro, A. C.; Rocha, Â.; Soares, R. M. D.; Fonseca, L. P.; da Silveira, N. P. Synthesis and Characterization of Acetylated Amylose and Development of Inclusion Complexes with Rifampicin. *Carbohydr. Polym.* **2017**, *157*, 267−274.
(26) Staiger, R.; Miller, E. B. Isatoic Anhydride. IV. Reactions with Various Nucleophiles. *J. Org. Chem.* **1959**, *24*, 1214−1219.
(27) de Belder, A. N.; Granath, K. Preparation and Properties of Fluorescein-Labelled Dextrans. *Carbohydr. Res.* **1973**, *30*, 375−378.
(28) Behzadi, S.; Serpooshan, V.; Tao, W.; Hamaly, M. A.; Alkawareek, M. Y.; Dreaden, E. C.; Brown, D.; Alkilany, A. M.; Farokhzad, O. C.; Mahmoudi, M. Cellular Uptake of Nanoparticles: Journey inside the Cell. *Chem. Soc. Rev.* **2017**, *46*, 4218−4244.

DOI: 10.1021/acsami.8b07450
ACS Appl. Mater. Interfaces 2018, 10, 30946−30951